Observations of aminium salts in atmospheric nanoparticles and possible climatic implications

James N. Smith[a,b,c,1], Kelley C. Barsanti[a], Hans R. Friedli[a], Mikael Ehn[d], Markku Kulmala[d], Donald R. Collins[e], Jacob H. Scheckman[f], Brent J. Williams[f], and Peter H. McMurry[f]

[a]Atmospheric Chemistry Division, National Center for Atmospheric Research, 1850 Table Mesa Dr., Boulder, CO 80305; [b]Department of Physics, University of Kuopio, P.O. Box 1627, 70211 Kuopio, Finland; [c]Finnish Meteorological Institute, Kuopio Unit, P.O. Box 1627, 70211 Kuopio, Finland; [d]Department of Physics, University of Helsinki, P.O. Box 64, 00014 Helsinki, Finland; [e]Department of Atmospheric Sciences, Texas A&M University, MS 3150, College Station, TX 77843; and [f]Particle Technology Laboratory, Department of Mechanical Engineering, University of Minnesota, 111 Church Street SE, Minneapolis, MN 55455

Edited by Barbara J. Finlayson-Pitts, University of California, Irvine, Irvine, CA, and approved November 25, 2009 (received for review October 20, 2009)

We present laboratory studies and field observations that explore the role of aminium salt formation in atmospheric nanoparticle growth. These measurements were performed using the Thermal Desorption Chemical Ionization Mass Spectrometer (TDCIMS) and Ultrafine Hygroscopicity Tandem Differential Mobility Analyzers. Laboratory measurements of alkylammonium—carboxylate salt nanoparticles show that these particles exhibit lower volatilities and only slightly lower hygroscopicities than ammonium sulfate nanoparticles. TDCIMS measurements of these aminium salts showed that the protonated amines underwent minimal decomposition during analysis, with detection sensitivities comparable to those of organic and inorganic deprotonated acids. TDCIMS observations made of a new particle formation event in an urban site in Tecamac, Mexico, clearly indicate the presence of protonated amines in 8–10 nm diameter particles accounting for about 47% of detected positive ions; 13 nm particles were hygroscopic with an average 90% RH growth factor of 1.42. Observations of a new particle formation event in a remote forested site in Hyytiälä, Finland, show the presence of aminium ions with deprotonated organic acids; 23% of the detected positive ions during this event are attributed to aminium salts while 10 nm particles had an average 90% RH growth factor of 1.27. Similar TDCIMS observations during events in Atlanta and in the vicinity of Boulder, Colorado, show that aminium salts accounted for 10–35% of detected positive ions. We conclude that aminium salts contribute significantly to nanoparticle growth and must be accounted for in models to accurately predict the impact of new particle formation on climate.

amine | atmosphere | new particle formation | Thermal Desorption Chemical Ionization Mass Spectrometer

The formation and growth of atmospheric nanoparticles, which are defined here as particles with diameters smaller than 50 nm, have been the object of intense study in recent years (1), due in large part to the potential role that new particle formation (NPF) may play in climate through the production and modification of cloud condensation nuclei (CCN). While models are beginning to provide information on the role that NPF plays in climate (2), the accuracy of such predictions is limited by our inadequate understanding of chemical processes that contribute to growth. Understanding growth mechanisms is essential because the growth rate determines whether a newly formed particle will ultimately grow to CCN size (~100 nm in diameter) or be scavenged by preexisting aerosol (3). Until recently, sulfuric acid (H_2SO_4) was the only species known to contribute to nanoparticle growth. However parallel measurements of nanoparticle growth rates (4) and H_2SO_4 (5) show that H_2SO_4 typically accounts for only 5% to 50% of the observed growth (6–8). This suggests that other species are contributing to postnucleation growth. These compounds must possess very low volatilities in order to overcome the Kelvin effect; very few known oxidation products of common volatile organic compounds satisfy this requirement (9).

The first direct observation of the organic species that contribute to growth was made in the Finnish boreal forest in 1999, where Mäkelä and colleagues found that nucleated particles were enriched with dimethylammonium (10). Recently, we reported direct measurements of the molecular composition of 8–30 nm diameter particles formed from nucleation during the Megacity Initiative: Local and Global Research Observations (MILAGRO) field study in Tecamac, Mexico (11), in which we observed that (a) organic compounds contributed to 90% of the observed growth of freshly nucleated particles and (b) some of the species that contributed to this organic fraction could belong to the class of aminium compounds, cations with the structure R_3NH^+ formed by protonation of an amine, with R being an alkyl group or H. In a subsequent article we hypothesized that amines can form organic salts with organic and inorganic acids in newly formed particles, and thus by transforming these species into ion pairs they would become essentially nonvolatile (12). One conclusion from that study was that aminium salt formation may exceed ammonium salt formation when total concentrations of gas-phase amines and ammonia levels are comparable. The reactive uptake of amines into bulk aerosol has been the subject of several studies recently. One laboratory study showed that trimethylamine at ~1 ppb displaces the ammonium in ammonium nitrate particles after exposure of a few hours (13). An extensive laboratory study of aliphatic amines focused on the roles of both salt formation and oxidation chemistry in gas-particle partitioning (14). That study confirmed that alkylammonium sulfate and nitrate salts could form and that gas-phase oxidation of the amine alkyl groups can lead to low-volatility oxidation products that can physically partition into particles. Recent field measurements have shown that aminium salt formation occurs in aged organic carbon particles in Riverside, California (15), and in the Central Valley region of California (16); both of these sites are downwind of bovine sources.

Organic salt formation from the reactive uptake of amines increases the effective van't Hoff factor of the solute, thereby decreasing the water vapor saturation required for a particle to develop into a CCN. A laboratory study of the reactive uptake of ammonia onto slightly soluble organic acid particles found that this process can significantly increase the CCN activity and hygroscopic growth of these particles (17). Since aminium ions form similar salts with deprotonated acids this result can be extended to the reactive uptake of amines. Thus, aminium salt formation

Author contributions: J.N.S., K.C.B., H.R.F., M.E., M.K., D.R.C., J.H.S., B.J.W., and P.H.M. designed research; J.N.S., K.C.B., H.R.F., M.E., M.K., D.R.C., J.H.S., B.J.W., and P.H.M. performed research; J.N.S., M.E., and D.R.C. analyzed data; and J.N.S. wrote the paper.

The authors declare no conflict of interest.

This article is a PNAS Direct Submission.

[1]To whom correspondence should be addressed. E-mail: jimsmith@ucar.edu.

may contribute to both haze and cloud droplet formation and to nanoparticle growth. The presence of particulate organic salts was raised as a possible explanation for the relatively high aerosol hygroscopicity and cloud condensation nuclei concentrations observed in the Amazon basin (18).

In summary, while it is recognized that amines can form extremely low volatility compounds within particles through the formation of salts with organic and inorganic acids, the Mäkelä et al. study from the Finnish boreal forest (10) and our study from MILAGRO that identified a possible aminium fragment ion (11) have provided the only observations to date that implicate amines in postnucleation growth. This scarcity of data is due in large part to the great difficulties inherent in measuring the composition of newly formed particles, which are characterized by mass loadings on the order of a million times lower than the accumulation mode and rapid timescales for formation and loss that require analysis times on the order of minutes. This manuscript reports on recent measurements made by the Thermal Desorption Chemical Ionization Mass Spectrometer (TDCIMS) (19, 20), an instrument specifically designed to determine the molecular species responsible for nanoparticle growth. We report TDCIMS and Ultrafine Hygroscopicity Tandem Differential Mobility Analyzer (UHTDMA) measurements during NPF events in two very different airsheds, Mexico City and the boreal forest at Hyytiälä Finland, that directly identify aminium ions as major constituents of ambient nanoparticles. We also summarize TDCIMS observations on the abundance of aminium ions in nanoparticles formed from nucleation in Atlanta and in and around Boulder, Colorado. These observations lead us to conclude that aminium salt formation is both widespread and could account for a significant part of nanoparticle growth by organics.

Results and Discussion

We carried out laboratory measurements to characterize the response of the UHTDMA and TDCIMS instruments to 8–20 nm diameter aminium salt particles formed from the following model compounds: methylamine (MA), dimethylamine (DMA), trimethylamine (TMA), acetic acid (AA), and propanoic acid (PA). Fig. 1*A* shows the volatility of 7.5 nm salt particles as a function of temperature, which we compare to previously published results for ammonium sulfate (21). Because theory predicts that for a given material and in the absence of significant curvature effects, the diameter decrease due to heating should be independent of size for particles that are much smaller than the mean free path of air (22), we express volatility as the decrease in particle diameter after heat treatment. Fig. 1*A* shows that aminium salts are less volatile than ammonium sulfate at temperatures above 80 °C and therefore are quite stable and represent a possible postnucleation growth pathway. Fig. 1*B* shows the hygroscopic growth, where the hygroscopic growth factor (HGF) is defined as the ratio of the diameter after exposure to 90% RH to the initial dry particle diameter, for the same model salt particles; once again these results are compared with published HGFs for ammonium sulfate nanoparticles (23). The hygroscopicities of the model salt particles all fall within a narrow range of values, which show a dependence on diameter due to the Kelvin effect. In general the amine salts are slightly less hygroscopic than ammonium sulfate, e.g., 1.20 ± 0.05 at 10 nm compared to 1.35 for ammonium sulfate at the same diameter.

The same model salt particles were analyzed with the TDCIMS to assess its ability to detect and quantify particulate amines, organic acids, and aminium salts. Regarding the organic acids, a recent study of the TDCIMS response to laboratory-generated four- to eight-carbon monocarboxylic and dicarboxylic acid particles concluded that the instrument could identify each by their deprotonated parent ion with minimal fragmentation, at sensitivities of *ca.* 100 Hz of integrated peak area per pg of collected aerosol mass (24). This is approximately equal to the instrument sensitivity toward sulfate in laboratory-generated ammonium sulfate aerosol (19). The main results obtained from these laboratory experiments were as follows: (a) individually, particulate amines and organic acids are both observed in the positive ion spectra as protonated parent ions, while in negative ion spectra organic acids are observed as deprotonated parent ions; (b) aminium salt particles are desorbed and ionized within the TDCIMS as if the amine and acid were independent from each other, that is, additional reactions between the desorbed species within the ion source such as those resulting in amide formation are not observed; (c) TDCIMS sensitivity towards particulate amines is equivalent to that of particulate organic acids. These studies, and the observations reported below, are based on reported ion abundances. While our results can be extended to particulate volume and thus actual diameter growth rates by estimating the average molar volumes of the aminium salts, this would require additional laboratory evaluations that are beyond

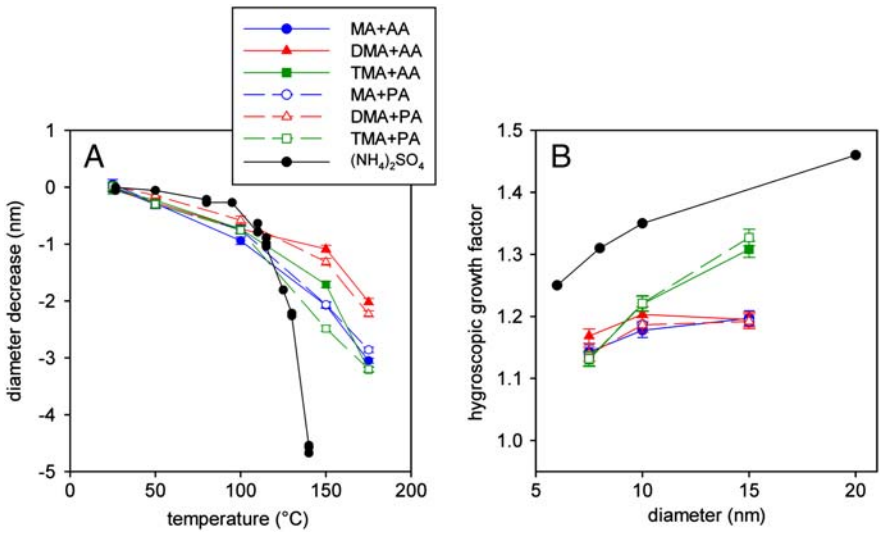

Fig. 1. Results of laboratory investigations of the volatility and hygroscopicity of aminium salt nanoparticles. MA: methylamine, DMA: dimethylamine, TMA: trimethylamine, AA: acetic acid, PA: propanoic acid. (*A*) Decrease in particle size versus temperature for 7.5 nm initial particle diameter. (*B*) Hygroscopic growth factor versus initial particle diameter at 90% RH.

the scope of our current investigations. For this study we can state more generally that a significant ion fraction of aminium salts implies a significant volume fraction, and thus a significant impact on nanoparticle growth.

We begin with a detailed analysis of two NPF events from two contrasting locales. The first event took place in Tecamac, Mexico (19.703N latitude, 98.982W longitude, 2273 m altitude), a mixed rural/urban site situated 40 km N of central Mexico City and heavily influenced by local rural sources as well as regional emissions, on March 21, 2006, during the MILAGRO field campaign (25). Fig. 2*A* shows a plot depicting the evolution of the particle size distribution function during the course of the event, where the black traces on this plot show the particle sizes analyzed by the TDCIMS. The diameter growth rate for this event was 20 nm hr^{-1} (4). This growth rate was used along with measurements of gaseous H_2SO_4 to estimate that H_2SO_4 contributed about 8% of the observed growth, a result that is consistent with nanoparticle composition measurements for a similar event that took place at the same location 4 d earlier (11). Therefore we can conclude from this analysis that organic compounds are responsible for over 90% of the growth observed in the Tecamac event.

Fig. 2*B* shows HGFs for 13 nm diameter particles. The HGF increased abruptly from a preevent value of about 1.2 to an average value during the event of 1.42 ± 0.02 (1σ). Fig. 2*C* shows the results of TDCIMS measurements of nanoparticle composition during the event. During the MILAGRO campaign, we acquired only positive or negative spectra on a given day because of the time required to reconfigure the instrument from one polarity to the other. For subsequent campaigns we redesigned the instrument to enable automatic polarity switching, thereby enabling near simultaneous measurements of positive and negative ion mass spectra. This is important because positive ion spectra enable quantification of species like the amines, while negative spectra enable quantification of the inorganic and organic acids. Therefore, dual polarity measurements enable more complete analyses. During the Tecamac event in which the TDCIMS obtained positive ion mass spectra, protonated MA and DMA dominate the spectra, comprising 40–50% of the total ions. Ammonium is seen as a trace ion, possibly due to exchange with aminium within particles as suggested by previous investigations. Other identified ions include protonated methanol and acetaldehyde, which are believed to be decomposition products of higher molecular weight oxidized organic species (11).

The second NPF event was observed during the European Integrated Project on Aerosol Cloud Climate and Air Quality Interactions 2007 campaign (26) at the SMEAR-II research station in Hyytiälä, Finland (61.850N latitude, 24.283W longitude, 181 m altitude). Fig. 3*A* shows the plot of the particle size distribution function, with a horizontal line marking the 10 nm TDCIMS analysis diameter during the event. Back trajectories calculated using the Hybrid Single Particle Lagrangian Integrated Trajectory (HYSPLIT, version 4) model show that the air mass associated with this event originated in the clean sector off the northwest coast of Norway, as is typical of NPF events in Hyytiälä. The average growth rate was 2.5 nm hr^{-1}, which is almost an order of magnitude lower than that of the Tecamac event. During this day the sulfuric acid concentration is around 2×10^6 cm^{-3} (27), from which we estimate that sulfuric acid uptake accounts

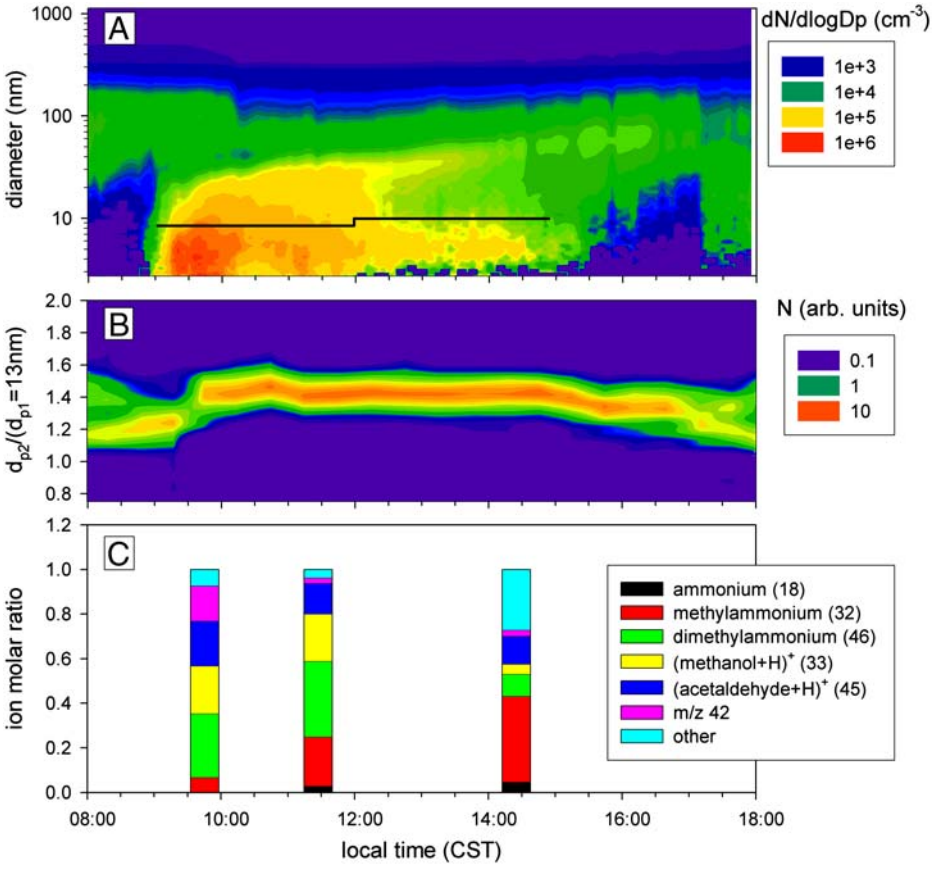

Fig. 2. Analysis of a new particle formation event commencing at 9:00 on March 21, 2006, in Tecamac, Mexico. (*A*) Particle size distribution intensity plot. Black lines mark the particle sizes that are analyzed by the TDCIMS. (*B*) Hygroscopic growth factors obtained at 90% RH for 13 nm ambient particles. (*C*) TDCIMS positive ion molecular composition for the diameters indicated in (*A*). Individual bar lengths correspond to the ion molar ratio, defined as the ratio of the average ion abundance for each compound to the total average ion abundance, and their width indicates sampling time. Average uncertainty for each species measurement is ±25%; refer to *Materials and Methods* for an uncertainty analysis.

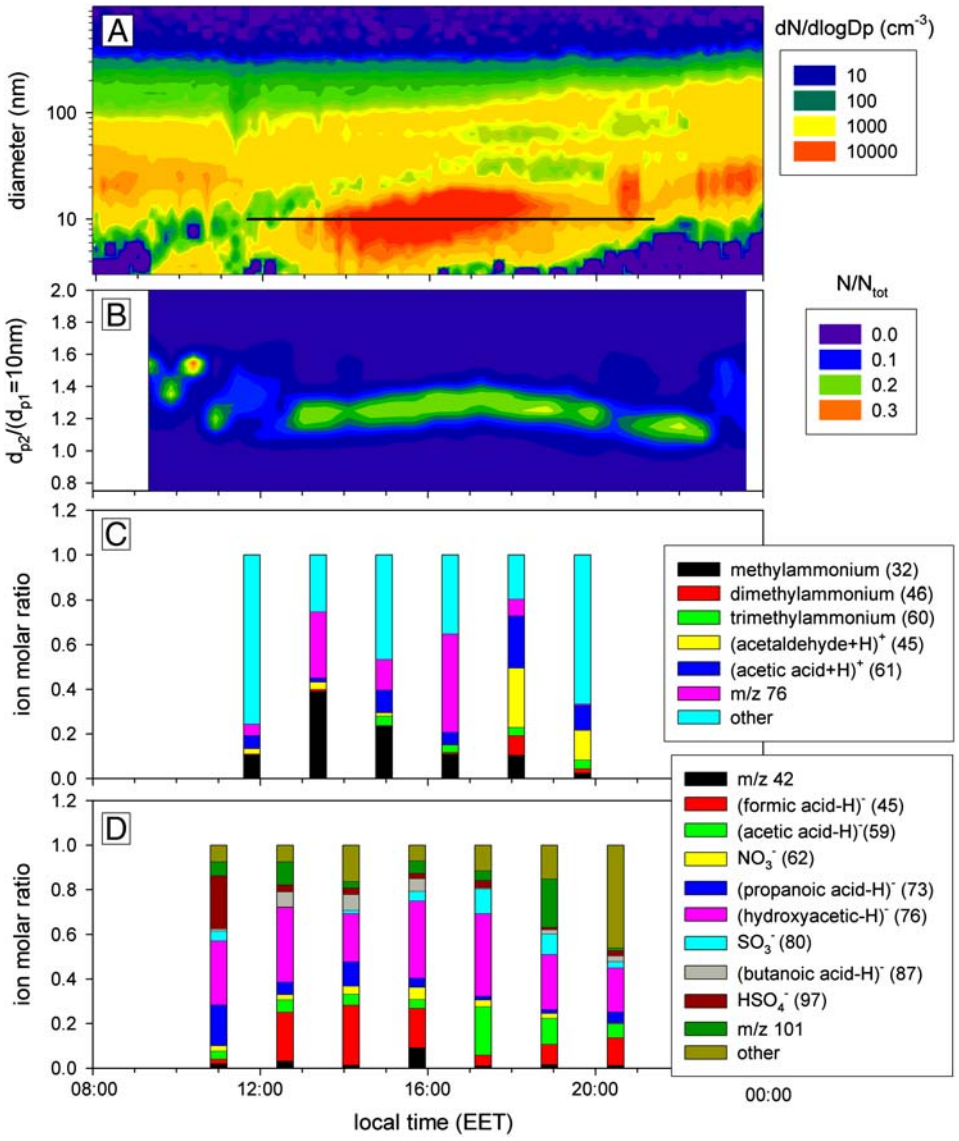

Fig. 3. Analysis of a new particle formation event commencing at 12:00 on April 9, 2007, in Hyytiälä, Finland. (*A*) Particle size distribution intensity plot. Black line marks the particle size that is analyzed by the TDCIMS. (*B*) Hygroscopic growth factors obtained at 90% RH for 10 nm ambient particles. (*C*) TDCIMS positive ion and (*D*) negative ion molecular composition for the diameter indicated in (*A*). Individual bar lengths correspond to the ion molar ratio, defined as the ratio of the average ion abundance for each compound to the total average ion abundance, and their width indicates sampling time. Average uncertainty for each species measurement is ±25%; refer to *Materials and Methods* for an uncertainty analysis.

for about 5% of the observed aerosol growth rate. This event also produced almost two orders of magnitude fewer particles compared to the Tecamac event.

Fig. 3*B* shows that the average HGFs for 10 nm diameter particles during the event is 1.27 ± 0.04 (1σ), slightly higher than previously published 10 nm diameter growth factors associated with clean NPF events at Hyytiälä (28). Data prior to the event show higher HGFs for 10 nm particles, likely associated with anthropogenic aerosol that advected to the site in the morning. This is supported by measurements of NO_x and SO_2, both of which reached their peak values in the morning with mixing ratios of 1.5 ppbv at 8:00 and 0.9 ppb at 3:00, respectively. HGFs following the event at 21:00 average 1.17, consistent with the growth factor of the lower diameter end of the Aitken mode from previous investigations (28). Fig. 3*C* and *D* show the results of TDCIMS measurements of positive and negative ion mass spectra obtained from nanoparticles collected during this event. The positive ion spectrum (Fig. 3*C*) includes signals at many masses, most of which are assumed organic but could not be easily identified. The peaks that could be identified were dominated by protonated MA, with minor peaks associated with protonated DMA and TMA. Near the end of the event, peaks corresponding to protonated acetaldehyde and acetic acid appeared. As mentioned above, these are likely decomposition products of oxidized particulate organics. The negative ion spectra (Fig. 3*D*) show that the aerosol contained a mixture of deprotonated organic acids and fragments of oxidized sulfur compounds. The latter appear in greater amounts prior to the event, which is consistent with elevated levels of SO_2 observed in the morning. The deprotonated organic acids observed include one- to four-carbon monocarboxylates, as well as the more highly oxidized deprotonated hydroxyacetic acid.

Fig. 4 summarizes our observations for the abundance of aminium salts in diverse sites where we've carried out TDCIMS measurements. This figure shows the aminium average ion ratio, which equals the average total aminium peaks divided by the average total nonacid peaks in the positive ion spectrum during NPF events. We chose to normalize by the sum of all positive

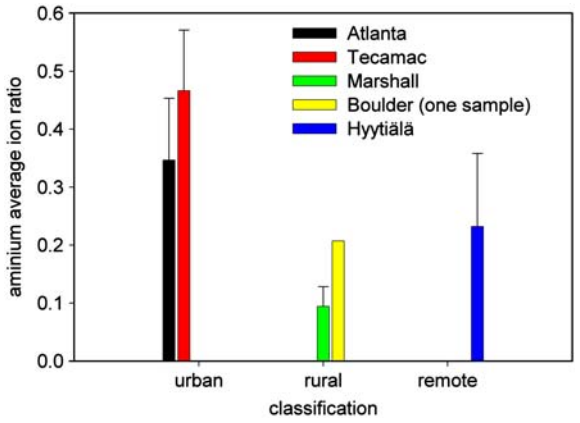

Fig. 4. Overview of the molar ratio of aminium salt formation during nanoparticle growth events, grouped according the land type, for representative events in which the TDCIMS performed measurements. Error bars indicate standard deviation of the mean.

ion nonacid peaks based on the assumption that most oxidized particulate organic compounds will be represented by a peak in this spectrum. Thus by dividing the aminium ion concentration by the sum of these peak areas, we are normalizing by the sum of species that reside in particles based on physical partitioning as well as through salt formation. We assume that observed aminium species are neutralized by deprotonated organic and inorganic acids, since the presence of such low molecular weight species in nanoparticles requires that these be ionized to suppress their vapor pressure. We recognize that there is still much debate as to the exact nature of the species that directly partition into atmospheric nanoparticles, and thus our accounting for their molar ratios in this way may lead to some systematic biases. Nonetheless, the data presented in Fig. 4 represents a reasonable first estimate of the impact of organic salt formation on nanoparticle composition. In addition to the data from Tecamac and Hyytiälä, we plot: an event that took place on July 24, 2009, during the Nucleation and CCN 2009 field campaign in Atlanta; a May 17, 2009, event taking place in north Boulder, Colorado; and a December 13, 2007, event taking place in Marshall, Colorado (29), a rural site located 6 km south of central Boulder, Colorado.

In the urban areas, aminium salt formation comprises almost half of the detected positive ions. As Figs. 2*C* and 3*C* show, these aminium ions usually appear as one- to three-carbon alkylammonium ions. Measurements in Boulder, Colorado, show that m/z 100.17 is the most abundant in the positive ion spectrum. One possible explanation for this is an ion with molecular formula $C_6H_{13}NH^+$, possibly protonated cyclohexylamine or methylpiperidine. Our observations clearly demonstrate the important role of organic salt formation on nanoparticle composition, ranging from 10% ion molar ratio in Marshall, Colorado, where ammonium is the dominant base, to 47% in Tecamac, Mexico. Measurements of aerosol hygroscopicity (Figs. 2*B* and 3*B*) show that the observed HGFs are higher than those obtained in the laboratory for pure aminium salts (Fig. 1*B*). This is consistent with observations because the ambient particles are not pure aminium salts but contain other compounds with hygroscopic moieties. High growth factors such as these are usually attributed to the presence of particulate inorganic compounds such as ammonium sulfate, whereas aged organic aerosol such as that produced from terpene oxidation typically exhibit growth factors of <1.1 for particles of this diameter (30). Organic salt formation provides one explanation for how a predominantly organic aerosol can also be hygroscopic.

The observations that we provide here represent the most complete characterization to date of the molecular composition of atmospheric nanoparticles. Taken together, the TDCIMS and UHTDMA results show that newly formed particles are a complex mixture in which ionized species such as aminium and carboxylates coexist with others that may possess very low vapor pressures and physically partition into particles. Ion molar ratios of 23% and 47% for Hyytiälä and Tecamac, respectively, suggest that salt formation can explain a significant amount of the observed growth due to organic compounds, which are estimated to be 92% and 95%, respectively, based on independent measurements of H_2SO_4 and particle growth rates. However, it is unlikely that organic salt formation accounts for all of the growth due to organic compounds. Assuming molar volumes to be approximately equal for all species, our measurements imply that organic salt formation can explain 23% and 47% of the observed growth Hyytiälä and Tecamac, respectively. Consequently, there is a need to understand the multiple mechanisms by which organics partition into particles, either reactively or physically. Our results suggest that such efforts will require parallel measurements of gas and particulate phase amines as well as inorganic and organic acids.

Materials and Methods

Laboratory-generated aminium salt nanoparticles were synthesized by mixing equal molarities of organic acids and bases (Sigma-Aldrich, >99% purity) in deionized and filtered water and electrospraying using a TSI 3480 electrospray aerosol generator. Particles were dehydrated through a heated sample inlet and analyzed using a nano-Tandem Differential Mobility Analyzer (n-TDMA) (31). In n-TDMA, ambient particles are neutralized with ^{210}Po diffusion charger and size selected using a nano-DMA (32). Quasi-monodispersed charged particles exiting the first nano-DMA are conditioned at a constant temperature or RH and then introduced into a second nano-DMA with an Ultrafine Condensation Particle Counter (33) where a size spectrum is obtained. For these laboratory experiments, volatility and hygroscopicity measurements were made for monocarboxylic acids (acetic acid $C_2H_4O_2$, propionic acid $C_3H_6O_2$) mixed with amine bases (methylamine CH_5N, dimethylamine C_2H_7N, trimethylamine C_3H_9N). Volatility measurements were made at 25 °C (near room temperature), 50 °C, 100 °C, 150 °C, and 175 °C, and hygroscopicity measurements were made at 90% RH. All n-TDMA data were processed using TDMAFIT (34).

The UHTDMAs used in Tecamac, Mexico (35), and Hyytiälä, Finland (36), were similar in design to that used in our laboratory studies, with the exception that they only measured aerosol hygroscopicity. Particle size distributions from Tecamac were obtained using a system of three particle sizing instruments that, combined, measure the particle number distribution every 5 min over the size range from 3 nm to 2 μm (37). Particle size distributions from Hyytiälä were obtained using a slightly different suite of instruments that covered a size range from 3 nm to 1 μm every 10 min (38).

Nanoparticle molecular composition in both laboratory and field experiments were obtained using the Thermal Desorption Chemical Ionization Mass Spectrometer (TDCIMS). The TDCIMS is an instrument capable of online measurements of the molecular composition of nanoparticles as small as 8 nm in diameter at time resolutions of 5 to 20 min (19, 20). The TDCIMS uses a low resolution electrostatic classification technique (39) to collect samples of aerosol nanoparticles on a metal filament and then resistively heats the filament and analyzes the desorbed gas using chemical ionization mass spectrometry. Samples were collected for 5 min in Tecamac and 15 min in Hyytiälä. During sample analysis, the desorption temperature was linearly ramped from room temperature to 500 °C over a period of 90 s while mass spectra were acquired. The upper temperature was selected to ensure desorption of nonrefractory constituents (40). Positive and negative ion mass spectra are created from the neutral species thermally desorbed from particles through either proton or electron transfer with $(H_2O)_nH^+$ or $(H_2O)_nO_2^-$ reagent ions, respectively, with n ranging from 1 to 4. The composition data are presented as ion molar ratio, which is the ratio of the average ion abundance for each ion to the total average ion abundance. A measurement uncertainty of ±25% is primarily associated with the uncertainty in calculating individual ion peak areas. This error is estimated based on the sampling time for individual ions and the total time required to obtain a full mass spectrum, which defines the dead time between sample points for the same ion.

ACKNOWLEDGMENTS. This research was supported by the Office of Science (BER), U.S. Department of Energy, grant DE-FG-02-05ER63997. The National Center for Atmospheric Research is operated by the University Corporation for Atmospheric Research under the sponsorship of the National Science Foundation. J.S. acknowledges financial support from the Saastamoinen Foundation.

1. Kulmala M, et al. (2004) Formation and growth rates of ultrafine atmospheric particles: A review of observations. *J Aerosol Sci*, 35:143–175.
2. Spracklen DV, et al. (2008) Contribution of particle formation to global cloud condensation nuclei concentrations. *Geophys Res Lett*, 35:L06808 doi:10.1029/2007GL033038.
3. Kuang C, McMurry PH, McCormick AV (2009) Determination of cloud condensation nuclei production from measured new particle formation events. *Geophys Res Lett*, 36:L09822 doi: 10.1029/2009GL037584.
4. Iida K, Stolzenburg MR, McMurry PH, Smith JN (2008) Estimating nanoparticle growth rates from size-dependent charged fractions—Analysis of new particle formation events in Mexico City. *J Geophys Res Atmos*, 113:D05207 doi: 10.1029/2007JD009260.
5. Eisele FL, Tanner DJ (1993) Measurement of the gas phase concentration of H_2SO_4 and methane sulfonic acid and estimates of H_2SO_4 production and loss in the atmosphere. *J Geophys Res*, 98:9001–9010.
6. Kulmala M, et al. (2001) On the formation, growth and composition of nucleation mode particles. *Tellus B*, 53:479–490.
7. Stolzenburg MR, et al. (2005) Growth rates of freshly nucleated atmospheric particles in Atlanta. *J Geophys Res Atmos*, 110:D22S05 doi: 10.1029/2005JD005935.
8. Wehner B, et al. (2005) The contribution of sulfuric acid and non-volatile compounds on the growth of freshly formed atmospheric aerosols. *Geophys Res Lett*, 32:L17810 doi: 10.1029/2005GL023827.
9. Kerminen VM, et al. (2000) Secondary organics and atmospheric cloud condensation nuclei production. *J Geophys Res Atmos*, 105:9255–9264.
10. Mäkelä JM, et al. (2001) Chemical composition of aerosol during particle formation events in boreal forest. *Tellus B*, 53:380–393.
11. Smith JN, et al. (2008) Chemical composition of atmospheric nanoparticles formed from nucleation in Tecamac, Mexico: Evidence for an important role for organic species in nanoparticle growth. *Geophys Res Lett*, 35:L04808 doi: 04810.01029/02007GL032523.
12. Barsanti KC, McMurry PH, Smith JN (2009) The potential contribution of organic salts to new particle growth. *Atmos Chem Phys*, 9:2949–2957.
13. Lloyd JA, Heaton KJ, Johnston MV (2009) Reactive uptake of trimethylamine into ammonium nitrate particles. *J Phys Chem*, 113:4840–4843.
14. Murphy SM, et al. (2007) Secondary aerosol formation from atmospheric reactions of aliphatic amines. *Atmos Chem Phys*, 7:2313–2337.
15. Pratt KA, Hatch LE, Prather KA (2009) Seasonal volatility dependence of ambient particle phase amines. *Environ Sci Technol*, 43:5276–5281.
16. Sorooshian A, et al. (2008) Comprehensive airborne characterization of aerosol from a major bovine source. *Atmos Chem Phys*, 8:5489–5520.
17. Dinar E, Anttila T, Rudich Y (2008) CCN activity and hygroscopic growth of organic aerosols following reactive uptake of ammonia. *Environ Sci Technol*, 42:793–799.
18. Mircea M, et al. (2005) Importance of the organic aerosol fraction for modeling aerosol hygroscopic growth and activation: A case study in the Amazon Basin. *Atmos Chem Phys*, 5:3111–3126.
19. Smith JN, Moore KF, McMurry PH, Eisele FL (2004) Atmospheric measurements of sub-20 nm diameter particle chemical composition by thermal desorption chemical ionization mass spectrometry. *Aerosol Sci Tech*, 38:100–110.
20. Voisin D, et al. (2003) Thermal desorption chemical ionization mass spectrometer for ultrafine particle chemical composition. *Aerosol Sci Tech*, 37:471–475.
21. Grose M, et al. (2006) Physical properties of ultrafine diesel exhaust particles sampled downstream of a catalytic trap. *Environ Sci Technol*, 40:5502–5507.
22. Sakurai H, et al. (2003) On-line measurements of diesel nanoparticle composition and volatility. *Atmos Environ*, 37:1199–1210.
23. Biskos G, et al. (2006) Prompt deliquescence and efflorescence of aerosol nanoparticles. *Atmos Chem Phys*, 6:4633–4642.
24. Smith JN, Rathbone GJ (2008) Carboxylic acid characterization in nanoparticles by thermal desorption chemical ionization mass spectrometry. *Int J Mass Spectrom*, 274:8–13.
25. Doran JC, et al. (2007) The T1-T2 study: Evolution of aerosol properties downwind of Mexico City. *Atmos Chem Phys*, 7:1585–1598.
26. Kulmala M, et al. (2009) Introduction: European Integrated Project on Aerosol Cloud Climate and Air Quality Interactions (EUCAARI)—Integrating aerosol research from nano to global scales. *Atmos Chem Phys*, 9:2825–2841.
27. Petaja T, et al. (2009) Sulfuric acid and OH concentrations in a boreal forest site. *Atmos Chem Phys*, 9:7435–7448.
28. Vaattovaara P, et al. (2009) The evolution of nucleation- and Aitken-mode particle compositions in a boreal forest environment during clean and pollution-affected new-particle formation events. *Boreal Environ Res*, 14:662–682.
29. Held A, Rathbone GJ, Smith JN (2009) A thermal desorption chemical ionization ion trap mass spectrometer for the chemical characterization of ultrafine aerosol particles. *Aerosol Sci Tech*, 43:264–272.
30. Virkkula A, Van Dingenen R, Raes F, Hjorth J (1999) Hygroscopic properties of aerosol formed by oxidation of limonene, alpha-pinene, and beta-pinene. *J Geophys Res Atmos*, 104:3569–3579.
31. Sakurai H, et al. (2005) Hygroscopicity and volatility of 4–10 nm particles during summertime atmospheric nucleation events in urban Atlanta. *J Geophys Res Atmos*, 110:D22S04 doi: 10.1029/2005JD005918.
32. Chen DR, et al. (1998) Design and evaluation of a nanometer aerosol differential mobility analyzer (Nano-DMA). *J Aerosol Sci*, 29:497–509.
33. Stolzenburg MR, McMurry PH (1991) An ultrafine aerosol condensation nucleus counter. *Aerosol Sci Tech*, 14:48–65.
34. Stolzenburg MR, McMurry PH (1988) *Tandem Differential Mobility Analyzer Fit (TDMAFIT) User's Manual* (Department of Mechanical Engineering, University of Minnesota, Minneapolis).
35. Gasparini R, et al. (2006) Application of aerosol hygroscopicity measured at the Atmospheric Radiation Measurement Program's Southern Great Plains site to examine composition and evolution. *J Geophys Res Atmos*, 111:D05S12 doi: 10.1029/2004JD005448.
36. Ehn M, et al. (2007) Hygroscopic properties of ultrafine aerosol particles in the boreal forest: Diurnal variation, solubility and the influence of sulfuric acid. *Atmos Chem Phys*, 7:211–222.
37. Woo KS, Chen DR, Pui DYH, McMurry PH (2001) Measurement of Atlanta aerosol size distributions: Observations of ultrafine particle events. *Aerosol Sci Tech*, 34:75–87.
38. Aalto P, et al. (2001) Physical characterization of aerosol particles during nucleation events. *Tellus B*, 53:344–358.
39. McMurry PH, et al. (2009) Sampling nanoparticles for chemical analysis by low resolution electrical mobility classification. *Environ Sci Technol*, 43:4653–4658.
40. Canagaratna MR, et al. (2007) Chemical and microphysical characterization of ambient aerosols with the Aerodyne aerosol mass spectrometer. *Mass Spectrom Rev*, 26:185–222.